

Shear Wave Velocity Determination for Site Subsoil Classification in New Zealand

Internship in Geophysics with the DAAD RISE Program
Celine Beier
01.06.2021 - 31.07.2021
Supervisor: Dr. Annika Greve

Contents

1	Introduction	2
2	Methods for Determining the Shear Wave Velocity V_S	2
3	Site Subsoil Classification	6
3.1	Site Subsoil Classification in New Zealand	6
3.2	Site subsoil classification in other countries	7
4	Seismic Cone Penetration Test Data	14
5	Shear Wave Velocity Profiles from SCPT Data	15
5.1	Data Analysis with the SPAS Software	15
5.1.1	Pre-Processing	15
5.1.2	Analysis modes	15
5.2	Data Analysis with Python	17
5.3	Comparison of the different analysis methods	23
6	Shear Wave Velocity Profiles from CPT-Data	25
7	Relation between Liquefaction and the Shear Wave Velocity	27
8	Horizontal-to-Vertical Spectral Ratio	30
	Bibliography	31

1 Introduction

Earthquakes create seismic body waves traveling through the earth in three dimensions as well as seismic surface waves spreading out along the Earth's surface around the epicentre. There are two types of seismic body waves, primary waves (also called compressional waves or P-waves) which are made up from compressions and expansions of soil particle moving forward and backward in the wave's direction, and shear waves (S-waves), where particles oscillate perpendicular to the propagation direction. The speed of a P-wave depends on the bulk modulus, shear modulus and density of the soil and is generally relatively fast with velocities up to $7\frac{km}{s}$ while the smaller S-wave velocity correlates only to the shear modulus and density. The ground shaking during an earthquake is governed by the shear wave velocity, the higher the velocity, the less ground shaking will occur. [1]

2 Methods for Determining the Shear Wave Velocity V_S

The different methods for determining the shear wave velocity V_S can be categorized into invasive and non-invasive methods. Invasive methods (table 1 and table 2) are considered to produce more reliable results, however, non-invasive methods are generally more inexpensive, faster to conduct and probe a greater soil volume, so they are more suitable to determine average properties. [2, 3] Non-invasive methods (table 3) rely on the analysis of the geometrical dispersion of surface waves: Surface waves with different frequencies have different velocities, in a soil profile where the wave velocity increases with depth smaller frequencies (longer wavelengths) correspond to higher wave velocities. The dispersion curve results from plotting the phase velocity versus the frequency. Surface wave analysis is based on measuring the dispersion curve (wave velocity versus frequency) and then calculating backwards which soil profile will create the measured dispersion function. [3]

Description	Advantages	Disadvantages
	Downhole Seismic Test (DH)[2, 4, 5]	
<ul style="list-style-type: none"> • borehole with seismic sensors at different depths • seismic wave is generated on the ground at some distance, detected by receivers, measurement of time gives velocity • methods to correct for refraction of waves at soil layers [5] 	<ul style="list-style-type: none"> • easy to use in sites where there already is a borehole, f.e. for construction or sample taking 	<ul style="list-style-type: none"> • needs a borehole • relies on assumptions regarding the wave path and the passed soil
	Seismic Cone Penetration Test (SCPT) [2, 4]	
<ul style="list-style-type: none"> • same principle as DH, but the receiver is build into a cone which is pushed into the soil • Cone Penetration Test (CPT) results are measured parallelly which can additionally be used for an estimate of V_s 	<ul style="list-style-type: none"> • less expensive than drilling a borehole • pushing the cone into the ground ensures a good coupling between the receiver and the ground 	<ul style="list-style-type: none"> • needs relatively soft soil to be able to push the cone in • relies on assumptions regarding the wave path and the passed soil
	Crosshole Seismic Test (CH) [2]	
<ul style="list-style-type: none"> • seismic wave source is lowered in one borehole, receivers are lowered into one or two other boreholes in a distance of 1.5-5m at the same depth • measurement of travel time gives velocity • source and receiver are moved to different depths to obtain a velocity profile 	<ul style="list-style-type: none"> • more reliable than DH as experimental uncertainties and the influence of depth effects can be minimized • when 2 receivers are used refracted wave paths and inhomogeneities in the soil can be detected 	<ul style="list-style-type: none"> • needs two or three boreholes • needs more time and equipment than DH - more expensive than DH • assumes straight wave travel path
	Direct Push Crosshole Test (DPCH) [2]	
<ul style="list-style-type: none"> • direct push equivalent of CH 	<ul style="list-style-type: none"> • see SCPT 	<ul style="list-style-type: none"> • see SCPT

Table 1: Invasive Tests I

Description	Advantages	Disadvantages
	P-S Suspension Logging [2]	
<ul style="list-style-type: none"> • borehole is filled with fluid, source is suspended in the fluid and creates a pressure wave which at the borehole wall is converted into P-and S-waves which travel upwards • receivers are suspended further up in the borehole and detect pressure waves when the seismic waves are converted back • time difference between the two receivers (usually 1m apart) gives velocity • lowering source and receiver allows for the determination of a velocity profile 	<ul style="list-style-type: none"> • can go to very high depths 	<ul style="list-style-type: none"> • needs a borehole • only characterises material in the immediate proximity of the borehole
	Standard Penetration Test (SPT) [2, 6]	
<ul style="list-style-type: none"> • V_S depends on material density and effective stress similar to the N-values determined in the SPT • V_S can be estimated from the measured N-values using a standard with known V_S and N-value (f.e. in [6]) 	<ul style="list-style-type: none"> • often and widely used • existence of databases • relatively inexpensive 	<ul style="list-style-type: none"> • no direct correlation between V_S and N-values - only estimates of V_S can be made

Table 2: Invasive Tests II

Description	Advantages	Disadvantages
	Spectral Analysis of Surface Waves (SASW) [3]	
<ul style="list-style-type: none"> source generates surface waves which are detected by two receivers at different distances from the source receivers record the phase shift dependent on the frequency - phase shift is related to the phase velocity which gives the dispersion curve 	<ul style="list-style-type: none"> non-invasive 	<ul style="list-style-type: none"> solutions for the velocity profile from the dispersion curves do not need to be unique
	Multichannel Analysis of Surface Waves (MASW) [3]	
<ul style="list-style-type: none"> source generates surface waves with are detected by multiple receivers distance - time relationship yields the dispersion curve via f.e. a double Fourier-transform 	<ul style="list-style-type: none"> non-invasive more receivers and data points give a more reliable result than SASW 	<ul style="list-style-type: none"> solutions do not need to be unique
	Refraction Microtremor (ReMi) [3]	
<ul style="list-style-type: none"> uses a passive source, several receivers are positioned in a 1D array analysis similar to MASW 	<ul style="list-style-type: none"> non-invasive passive source 	<ul style="list-style-type: none"> solutions do not need to be unique rely on homogenous distribution of wave sources only 1D profile
	Two-Dimensional Arrays [3]	
<ul style="list-style-type: none"> 2D equivalent of ReMi 	<ul style="list-style-type: none"> non-invasive passive source 	<ul style="list-style-type: none"> solutions do not need to be unique
	Horizontal-To-Vertical Spectral Ratio (HVSR) [3]	
<ul style="list-style-type: none"> allows for the determination of the fundamental resonance frequency of a site, which yields V_s when compared with the depth of the soil 	<ul style="list-style-type: none"> non-invasive inexpensive 	<ul style="list-style-type: none"> relies on estimates about f.e. depth to bedrock

Table 3: None-Invasive Tests

Class	Description	Definition
A	Strong Rock	UCS > 50 MPa & Vs30 > 1500 m/s & not underlain by < 18 MPa or Vs 600 m/s materials.
B	Rock	1 < UCS < 50 MPa & Vs30 > 360 m/s & not underlain by < 0.8 MPa or Vs 300 m/s materials, a surface layer no more than 3 m depth (HW-CW rock/soil).
C	Shallow Soil	not class A, B or E, low amplitude natural period $\leq 0.6s$, or depths of soils not exceeding those in Table 2.
D	Deep or Soft Soil	not class A, B or E, low amplitude natural period $> 0.6s$, or depths of soils exceeding those in Table 2, or underlain by < 10 m soils with undrained shear strength < 12.5 KPa, or < 10 m soils SPT N < 6.
E	Very Soft Soil	> 10m soils with undrained shear strength < 12.5 KPa, or > 10m soils with SPT N < 6, or > 10m soils with Vs ≤ 150 m/s, or > 10m combined depth of previous properties.

Figure 1: Site subsoil classification in New Zealand, from [6]. ¹

3 Site Subsoil Classification

3.1 Site Subsoil Classification in New Zealand

The velocity of an earthquake wave determines the ground shaking and depends on the soil the wave is moving through. Site subsoil testing aims to characterise the properties of the soil in order to predict the site's behaviour during an earthquake. The results can be included into the structural design to minimize the damage from an earthquake. [1, 7] In New Zealand, the geological site characteristics are included in the building design through different structural requirements determined in the New Zealand Buildings Code which references standards defined by Standards New Zealand. In NZS 1170.5:2004 five different subsoil classes are defined (class A-E, see figure 1) by the respective shear wave velocity, compressive strength, depth of soils and underlying materials. The preferred method for site classification is through the determination of site periods (4 times the shear wave travel-time through the material to the surface of the bedrock). If the classification via V_s is not possible, the soil can be classified by the measurement of geotechnical properties of the soil, the determination of the soil composition from boreholes or from the surface geology and estimates. [8]

¹UCS - unconfined compressive strength

HW - highly weathered

CW - completely weathered

SPT - Standard Penetration Test

3.2 Site subsoil classification in other countries

US [9, 10]

- 2012 International Building Code (IBC) describes building design regulations, it references the American Society of Civil Engineering Standard 7, Minimum Design Loads for Building and Other Structures (ASCE, 2010)
- ASCE defines 5 categories (see figure 2)
- alternatively: National Earthquake Hazards Reduction Program (NEHRP) provides a classification that is very similar (see figure 3)
- determination of the soil category by V_{S30} (average shear wave velocity over the upper 30m) or N-value (average standard penetration resistance) or average undrained shear strength
- IBC and NEHRP are also widely used in other countries (f.e. in [11] in Thailand or in [12] in India)

Canada [13]

- soil classification and design actions regulated in the National Buildings Code of Canada, 2005
- classification via average V_S (if not possible then penetration resistance or undrained shear strength)
- soil classes in figure 4

Europe [14, 15]

- Eurocode 8: Design of structures for earthquake resistance - defines construction standards in Europe
- site subsoil classification is defined in European Standard EN 1998-1, 2004
- intended to be a Europe-wide standard which is complemented by national additions (National Annex)
- study on the implementation in 2018 in [15], summary: Eurocode is widely accepted, often there is no additional national standard, if there is one, the Eurocode are only complemented with national standards as intended
- example for national standard: Italy with the Italian Building Code ItBC2018 which also accounts for the depth to bedrock in addition to V_{S30} and has a slightly different classification system refining the Eurocode system [16]
- preferred method of classification in the Eurocode is V_{S30} , soil classes in figure 5
- some methods used for V_S determination: MASW (f.e. in [17]), ReMi (f.e. in [16]), DH (f.e. in [16]) and CH (f.e. in [16])

Switzerland [18]

- Baugrundklassen defined in SIA 261 from 2014
- site classes A-F (figure 6), categorisation by shear wave velocity, but also N-value and undrained shear strength if those measurements exist

China [19]

- Code for Seismic Design of Buildings, GB 50011-2010
- the site is classified into one of four final categories: favorable, common, unfavorable, hazardous
- to classify a site into one of those 4 categories, the shear-wave velocity needs to be determined and the thickness of the soil layer has to be included
- the method for the shear wave velocity determination is not specified, only that the shear wave velocity needs to be measured in at least 3 boreholes per site
- the shear wave velocity can also be estimated by the type of soil

India [20]

- Indian Standards IS 1893 from 2002
- 3 soil classes defined by the soil type and N-value (figure 8)
- soil classification is often based on experience, no scientific guidelines
- since the classification in IS 1893 is rather ambiguous and outdated, other classification systems like the Eurocode, IBC or NEHRP are widely used [12]

Bolivia [21]

- site subsoil classification and building code in Norma Boliviana de diseño sísmico NBDS from 2006 (there wasn't any building code relating to seismic activity in Bolivia before that)
- classification preferably via V_{S30} , alternatively using N_{60}
- no preferred method for the determination of V_{S30} described
- soil classes in figure 9, the definitions are the same as for the site classes A-E in Canada

Table 20.3-1 Site Classification

Site Class	\bar{v}_s	\bar{N} or \bar{N}_{ch}	\bar{s}_u
A. Hard rock	$>5,000$ ft/s	NA	NA
B. Rock	2,500 to 5,000 ft/s	NA	NA
C. Very dense soil and soft rock	1,200 to 2,500 ft/s	>50	$>2,000$ psf
D. Stiff soil	600 to 1,200 ft/s	15 to 50	1,000 to 2,000 psf
E. Soft clay soil	<600 ft/s	<15	$<1,000$ psf
F. Soils requiring site response analysis in accordance with Section 21.1	Any profile with more than 10 ft of soil having the following characteristics: —Plasticity index $PI > 20$, —Moisture content $w \geq 40\%$, —Undrained shear strength $\bar{s}_u < 500$ psf		
	See Section 20.3.1		

For SI: 1 ft/s = 0.3048 m/s; 1 lb/ft² = 0.0479 kN/m².

Figure 2: Site Classification in the US according to ASCE 2010, from [9]

- A Hard rock with measured shear wave velocity, $\bar{v}_s > 5,000$ ft/sec (1500 m/s)
- B Rock with $2,500$ ft/sec $< \bar{v}_s \leq 5,000$ ft/sec (760 m/s $< \bar{v}_s \leq 1500$ m/s)
- C Very dense soil and soft rock with $1,200$ ft/sec $< \bar{v}_s \leq 2,500$ ft/sec (360 m/s $< \bar{v}_s \leq 760$ m/s) or with either $\bar{N} > 50$ or $\bar{s}_u > 2,000$ psf (100 kPa)
- D Stiff soil with 600 ft/sec $\leq \bar{v}_s \leq 1,200$ ft/sec (180 m/s $\leq \bar{v}_s \leq 360$ m/s) or with either $15 \leq \bar{N} \leq 50$ or $1,000$ psf $\leq \bar{s}_u \leq 2,000$ psf (50 kPa $\leq \bar{s}_u \leq 100$ kPa)
- E A soil profile with $\bar{v}_s < 600$ ft/sec (180 m/s) or with either
 $\bar{N} < 15$, $\bar{s}_u < 1,000$ psf, or any profile with more than 10 ft (3 m) of soft clay defined as soil with $PI > 20$, $w \geq 40$ percent, and $s_u < 500$ psf (25 kPa)
- F Soils requiring site-specific evaluations:
 1. Soils vulnerable to potential failure or collapse under seismic loading such as liquefiable soils, quick and highly sensitive clays, collapsible weakly cemented soils.
 - Exception:** For structures having fundamental periods of vibration less than or equal to 0.5 second, site-specific evaluations are not required to determine spectral accelerations for liquefiable soils. Rather, the Site Class may be determined in accordance with Sec. 3.5.2, assuming liquefaction does not occur, and the corresponding values of F_a and F_v determined from Tables 3.3-1 and 3.3-2.
 2. Peat and/or highly organic clays ($H > 10$ ft [3 m] of peat and/or highly organic clay, where H = thickness of soil)
 3. Very high plasticity clays ($H > 25$ ft [8 m] with $PI > 75$)
 4. Very thick, soft/medium stiff clays ($H > 120$ ft [36 m]) with $s_u < 1,000$ psf (50 kPa)

Figure 3: Site classification in the US according to NEHRP from [10]

Site Class	Ground Profile Name	Average Properties in Top 30 m, as per Appendix A		
		Average Shear Wave Velocity, \bar{V}_s (m/s)	Average Standard Penetration Resistance, \bar{N}_{60}	<i>Soil</i> Undrained Shear Strength, s_u
A	Hard rock	$\bar{V}_s > 1500$	n/a	n/a
B	Rock	$760 < \bar{V}_s \leq 1500$	n/a	n/a
C	Very dense <i>soil</i> and soft rock	$360 < \bar{V}_s < 760$	$\bar{N}_{60} > 50$	$s_u > 100$ kPa
D	Stiff soil	$180 < \bar{V}_s < 360$	$15 \leq \bar{N}_{60} \leq 50$	50 kPa $< s_u \leq 100$ kPa
E	Soft soil	$\bar{V}_s < 180$	$\bar{N}_{60} < 15$	$s_u < 50$ kPa Any profile with more than 3 m of <i>soil</i> with the following characteristics: <ul style="list-style-type: none"> • plasticity index: PI > 20 • moisture content: w $\geq 40\%$, and • undrained shear strength: $s_u < 25$ kPa
F	Other soils ⁽¹⁾	Site-specific evaluation required		

Figure 4: Site classification for Seismic Site Response in Canada, from [13]

Ground type	Description of stratigraphic profile	Parameters		
		$v_{s,30}$ (m/s)	N_{SPT} (blows/30cm)	c_u (kPa)
A	Rock or other rock-like geological formation, including at most 5 m of weaker material at the surface.	> 800	—	—
B	Deposits of very dense sand, gravel, or very stiff clay, at least several tens of metres in thickness, characterised by a gradual increase of mechanical properties with depth.	360 – 800	> 50	> 250
C	Deep deposits of dense or medium-dense sand, gravel or stiff clay with thickness from several tens to many hundreds of metres.	180 – 360	15 - 50	70 - 250
D	Deposits of loose-to-medium cohesionless soil (with or without some soft cohesive layers), or of predominantly soft-to-firm cohesive soil.	< 180	< 15	< 70
E	A soil profile consisting of a surface alluvium layer with v_s values of type C or D and thickness varying between about 5 m and 20 m, underlain by stiffer material with $v_s > 800$ m/s.			
S_1	Deposits consisting, or containing a layer at least 10 m thick, of soft clays/silts with a high plasticity index ($PI > 40$) and high water content	< 100 (indicative)	—	10 - 20
S_2	Deposits of liquefiable soils, of sensitive clays, or any other soil profile not included in types A – E or S_1			

Figure 5: Site classification in Europe according to EN 1998-1, from [14]

Baugrund-klasse	$V_{s,30}$ [m/s]	N_{SPT}	S_u [kPa]	Beschreibung
A	>800	-	-	Fels oder andere felsähnliche geologische Formation mit höchstens 5 m Lockergestein an der Oberfläche.
B	500–800	>50	>250	Ablagerungen von sehr dichtem Sand, Kies oder sehr steifem Ton mit einer Mächtigkeit von mindestens einigen zehn Metern, gekennzeichnet durch einen allmählichen Anstieg der mechanischen Eigenschaften mit der Tiefe.
C	300–500	15–50	70–250	Ablagerungen von dichtem oder mitteldichtem Sand, Kies oder steifem Ton mit einer Mächtigkeit von einigen zehn bis mehreren hundert Metern.
D	<300	<15	<70	Ablagerungen von lockerem bis mitteldichtem kohäsionslosem Lockergestein (mit oder ohne einige weiche kohäsive Schichten), oder von vorwiegend weichem bis steifem kohäsivem Lockergestein.
E	-	-	-	Oberflächliche Schicht von Lockergestein mit v_s -Werten nach C oder D und veränderlicher Dicke zwischen 5 m und 20 m über einem Bodenmaterial mit $v_s > 800$ m/s.
F	-	-	-	Strukturempfindliche, organische und sehr weiche Ablagerungen (z. B. Torf, Seekreide, weicher Lehm) mit einer Mächtigkeit über 10 m.

N_{SPT} erforderliche Schlagzahl für eine Eindringtiefe von 0,3 m bei einem Standard-Penetrometer test
 S_u Scheinbare undrainierte Kohäsion
 $V_{s,30}$ Mittlere Scherwellengeschwindigkeit bis in eine Tiefe von 30 m

Figure 6: Site subsoil classification in Switzerland, from [18]

Section type	Geological, topographical and geomorphic description
Favorable section	Stable rock bed, stiff soil, or wide-open, even, compacted and homogeneous medium-stiff soil
Common section	Sections not belonging to the favorable, unfavorable and hazardous sections
Unfavorable section	Soft soil, liquefied soil; stripe-protruding spur; lonely tall hill, steep slopes, steep step, river bank or boundary of side slopes, soil layer having obviously heterogeneous cause of formation, rock character and state in plane (including abandoned river beds, loosened fracture zone of fault, and hidden swamp, creek, ditch and pit, as well as base formatted with excavated and filled), plastic loess with high moisture, ground surface with structural fissure, etc
Hazardous section	Places where landslide, collapse, land subsidence, ground fissure and debris flow may occur during the earthquake, as well as the positions in causative fault where ground dislocation may occur

Figure 7: Site subsoil classification in China, from [19]

Type of Soil Mainly Constituting the Foundation

<i>Type I Rock or Hard Soil :</i>	<i>Type II Medium Soils :</i>	<i>Type III Soft Soils :</i>
Well graded gravel and sand gravel mixtures with or without clay binder, and clayey sands poorly graded or sand clay mixtures (GB, CW, SB, SW, and SC) ¹⁾ having $N^2)$ above 30, where N is the standard penetration value	All soils with N between 10 and 30, and poorly graded sands or gravelly sands with little or no fines (SP ¹⁾) with $N > 15$	All soils other than SP ¹⁾ with $N < 10$

Figure 8: Site subsoil classification in India, from [20]

Suelo	Descripción
S0	Roca dura
S1	Roca
S2	Suelo muy rígido - roca blanda
S3	Suelo rígido
S4	Suelo blando
S5	Requiere un análisis de respuesta de sitio

Figure 9: Site subsoil classification in Bolivia, from [21]

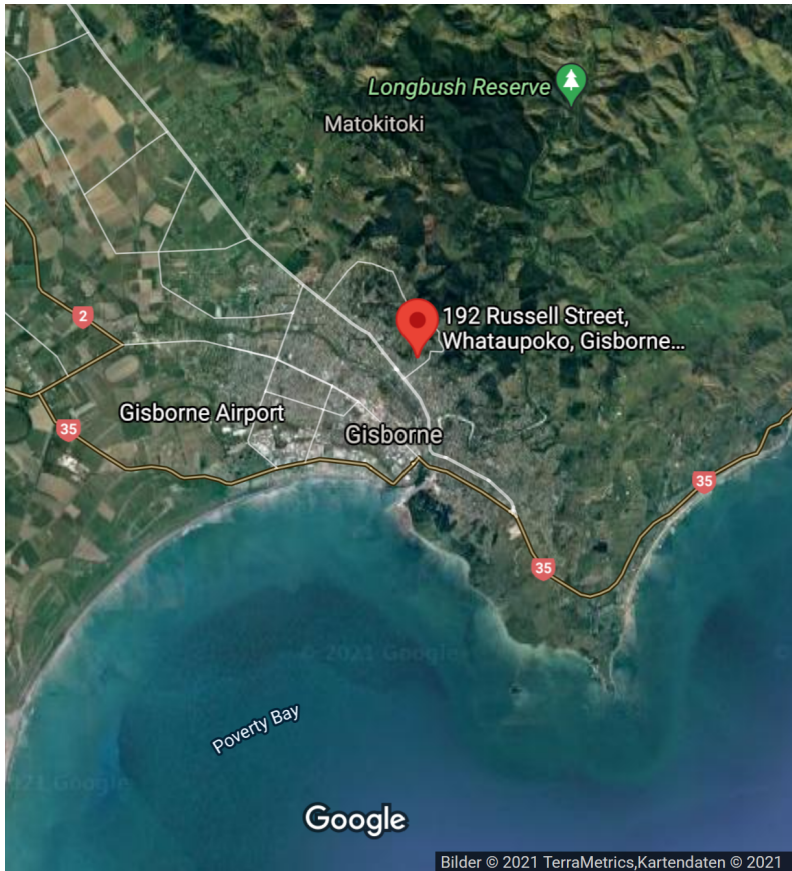


Figure 10: The site of data collection at 192 Russel Street in Gisborne, from [26].

4 Seismic Cone Penetration Test Data

The SCPT data was collected at 192 Russel Street, Gisborne (figure 10) by LDE Land Development and Engineering Ltd. The site is underlain by Holocene alluvial deposits (gravel, sand and silt). [22] The measured sleeve friction f_s and the cone resistance q_c can be correlated to yield the predictive soil behaviour type [23] which suggests clays between a depth of 1.5m and 7.5m, followed by silt mixtures with small layers of sands up to a depth of 12.5m. The liquefaction vulnerability is estimated to be moderate, meaning that during an earthquake minor changes in the ground structure and moderate structural damage can be expected. [24, 25]

5 Shear Wave Velocity Profiles from SCPT Data

5.1 Data Analysis with the SPAS Software

The SPAS software ² can be used to analyse the measured SCPT data in order to obtain a depth-shear wave velocity profile via different pre-processing and data analysis procedures:

5.1.1 Pre-Processing

The pre-processing steps include options to

- view the events in the time and frequency domain
- cut the signal length
- exclude faulty measurements - The events can be shown in a depth-travel time diagram (figure 11) from which the shear wave velocity can be obtained as the slope along the data points. Outliers can be an indication for erroneous data acquisition, for example when the depth information was not correctly noted down. Those events are then excluded from the following analysis to not distort the shear wave velocity calculation.
- filter the events - There are several options of filtering the events, however some filters introduce additional peaks or shift the signal peaks on the time axis which should be avoided. Figure 12 shows two different filtering options. The resulting shear wave velocities are depending on the applied filters, for the following steps no filter is applied as filtering seems to introduce additional uncertainties instead of providing an improvement of the analysis.

5.1.2 Analysis modes

The wave signal created on the surface propagates through the soil and the sensors at different depths will register the signal at different times (figure 13). The shear wave velocity profile can be calculated automatically by the software, however, the resulting velocities might display some extreme values that are in obvious disagreement with the measurement and are probably the result from a calculation error, for example when the software does not recognize the correct peak that is propagating through the soil and correlates with the arrival from a P- rather than a S-wave. It is then possible to manually correct individual velocity values by providing the software two points from successive signals which are then used to re-calculate the shear wave velocity. Besides this automatic and semi-automatic option of calculating the shear wave velocity, the software also allows to manually pick arrivals in each signal which are then used as the input for the velocity calculation. A comparison between those three methods can be seen in figure 17, the shear wave velocity calculation conducted with the arrivals picked by hand seems to be the most reliable method as the velocity profile shows the least miscalculations (depths with high calculated

²Seismic Analysis Software SPAS 2019 v.4.0 from Geologismiki

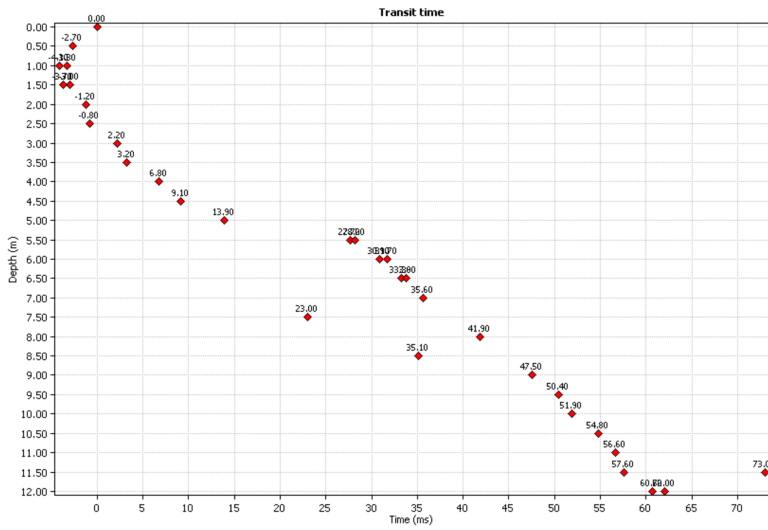


Figure 11: Depth - travel time diagram created with the SPAS software [27], used to identify faulty measurements.

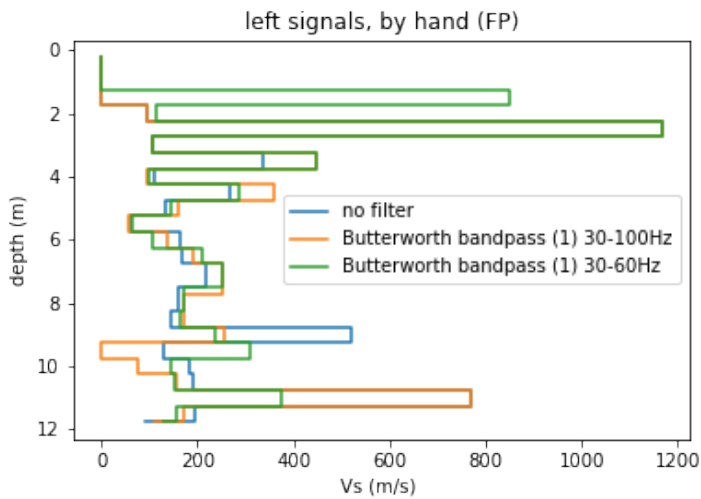


Figure 12: Depth - shear wave velocity profiles obtained with different filters.

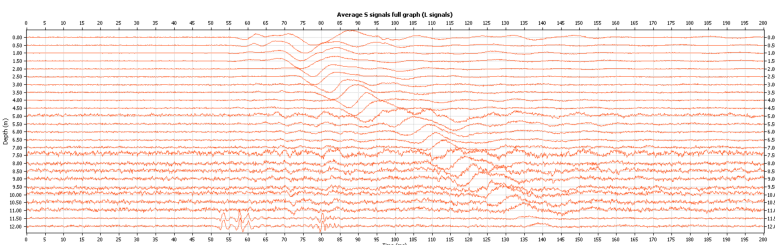


Figure 13: Depth - time diagram with the individual measurements showing the propagation of the wave through the soil from the SPAS software [27].

shear wave velocity that seems highly unlikely given the surrounding lower velocities). This method also allows for the most control over the analysis process as the automatic and semi-automatic method partially rely on the internal operations of the software that are not made transparent.

The velocity profiles can be calculated using only the data sets from one side (left or right) or using the mean of both sides. In theory, using the mean shear wave velocity for a certain depth from two measurements could help in dealing with single miscalculated velocities, for example due to misidentified peaks, as those values would be averaged out. Figure 19 compares the three methods using the signals from only the left side of the receiver and an average of the left and right side. Surprisingly, the shear wave velocities calculated using the mean of left and right signals more often than not show higher deviations from the expected values. A possible reason might be that miscalculations might add up instead of canceling each other out, in basically the opposite effect of what was hoped for. But it is far more likely that the measurements for the right side are not as reliable as the measurement setup was not ideal for the data acquisition.

When determining the shear wave velocity profile by hand, different points in the signal can be used as a reference, for example the first signal that arrives (FS, figure 14), the first peak (FP, figure 15) or the first cross-over (CO, figure 16) after the first peak. [28] Those methods are compared in figure 18. While selecting the reference point in the individual signals it was very hard to determine the arrival of the first signal, mostly because of background noise in the signal. Accordingly, the obtained velocity profile shows the largest deviations between the shear wave velocity estimates. In contrast, the determination of the first peak or the first cross-over was more straight forward. However, the calculations using the first arriving peak seem to have the least largest differences between the V_S estimates made, and in addition this method also seems to be the most easy to implement.

In summary, the SPAS software offers a lot of different methods for data pre-processing and analysis which will yield very varying results. Figure 20 shows a summary of all different analysis methods described above to show the huge variations in the resulting velocity profiles. Combining all those profiles gives an idea of what the actual profile might look like as individual large differences in the V_S estimates at single depths in the individual methods stand out more in comparison. Unfortunately, the SPAS software does not come with a description of the internal algorithms, which for example are used for the automatic velocity profile calculation, so it is difficult to trace the method and identify the sources for miscalculations. Given the comparisons made above, I think the most reliable and reproducible, although most time consuming, method would be to individually pick the first peak of the unfiltered signal by hand.

5.2 Data Analysis with Python

The measurements can also be analysed using a cross correlation function implemented in python, the direct method thereby relies on a cross correlation between the first measurement taken at the ground surface and every following measurement. Since only two measurements are taken at the same time, this method might

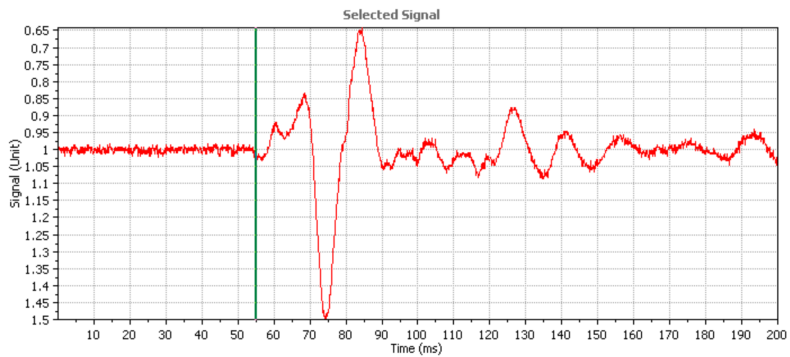


Figure 14: Single signal with the time of the first signal (FS) marked in the SPAS software [27],

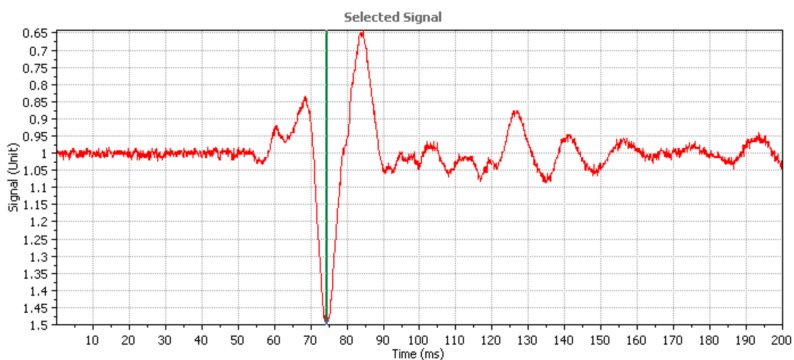


Figure 15: Single signal with the first peak (FP) marked in the SPAS software [27].

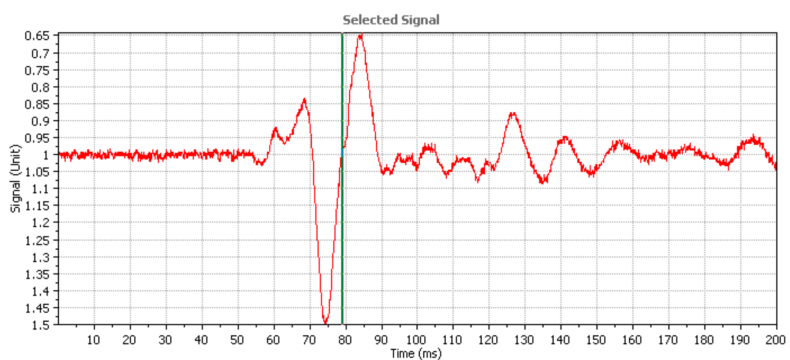


Figure 16: Single signal with the first cross-over (CO) marked in the SPAS software [27].

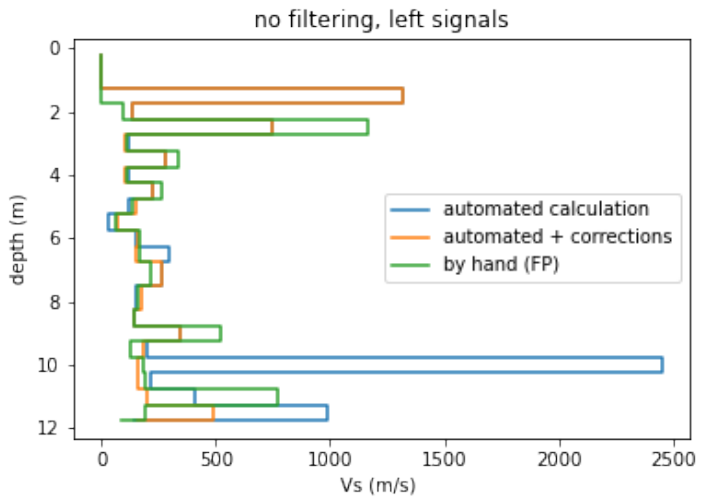


Figure 17: Depth - shear wave velocity profiles obtained by the automatic, semi-automatic and manual method (first peak) with the SPAS software [27].

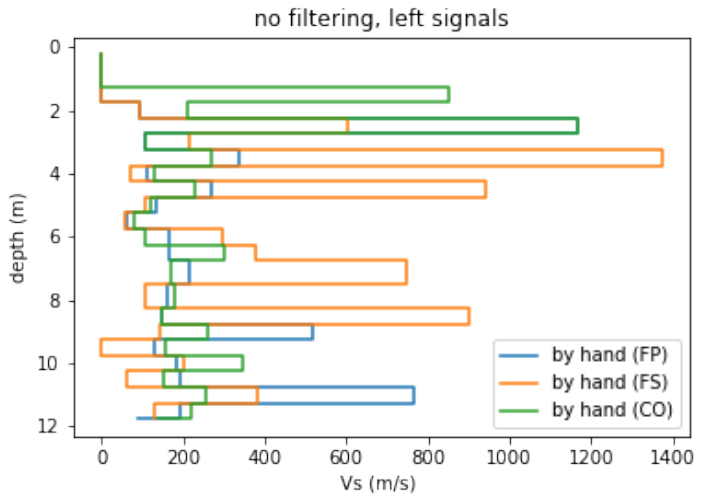


Figure 18: Depth - shear wave velocity profiles obtained by hand with different reference points: FP - first peak, FS - first signal, CO - first cross-over in the SPAS software [27].

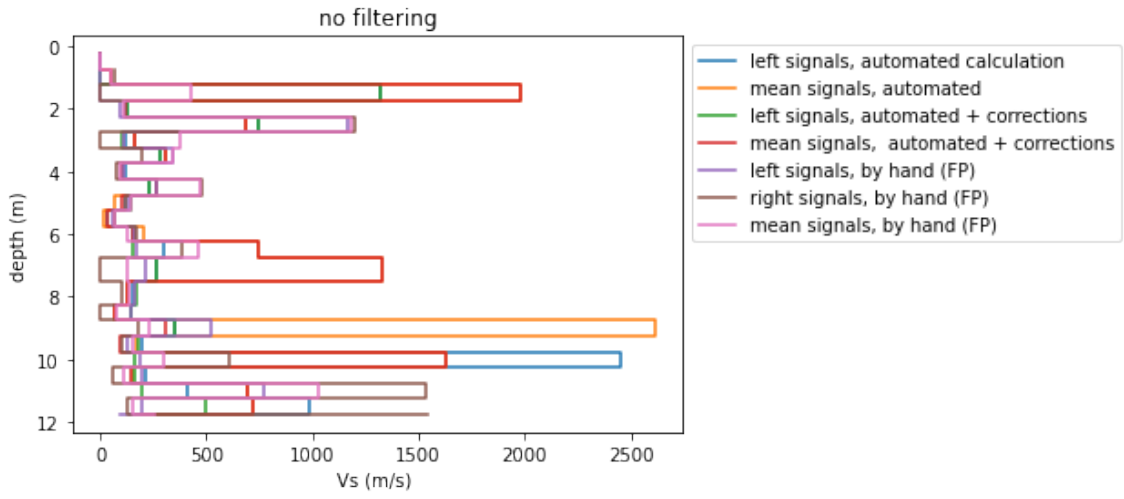


Figure 19: Depth - shear wave velocity profiles obtained by the automatic, semi-automatic and manual method (first peak) of the SPAS software [27] using only the signals from the left side and the mean signals.

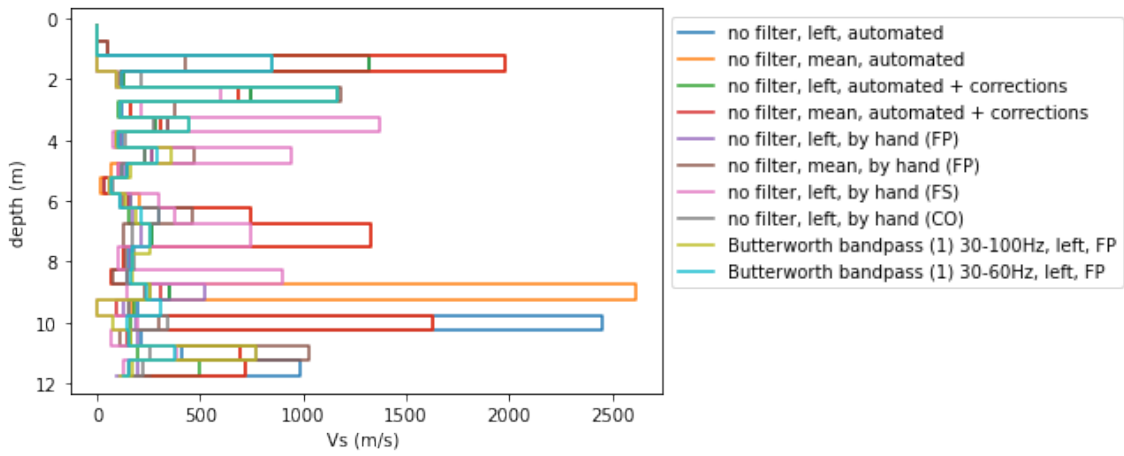


Figure 20: Different depth - shear wave velocity profiles obtained with the SPAS software [27].

be prone to additional errors, for example from differences in the time triggering between successive measurements. In contrast, the interval method relies on a cross correlation between the two measurements taken together which eliminates all error arising from differences between two data taking runs. In both the direct and interval method, the cross correlation yields the time difference between the two signals. Taking into account the differences in height, the shear wave velocity can be calculated. Figure 21 compares the resulting shear wave velocity profiles. Overall, direct and interval method agree well with each other up to a depth of 5m. At higher depths, the interval method shows significantly higher shear wave velocities which might be due to the inhomogenous composition of the ground comprised of layers of different soils. The interval method covering only 0.5m of depth difference might be more sensitive to those layers with different shear wave velocities than the direct method with a lower resolution.

Another possibility of determining the shear wave velocity is the slope method. Instead of individually calculating the velocity from the time difference between two signals, the travel time is plotted against the depths. In this diagram, linear functions are fitted to the data points, the slope of each linear function equals the shear wave velocity. This approach holds the advantage that the shear wave velocity is not determined in 0.5m intervals, but in bigger layers that might more accurately represent the soil composition. Each layer only gets one shear wave velocity and measurement errors between individual measurements are averaged out by the fit. On the other hand, the slope method relies on a manual determination of which points are used to fit which slope, and it might not be always clear, where the borders between two connecting linear fits lie. To test the slope method it is used on depths - travel time data obtained from the SPAS software and the direct method cross correlation. The fitted linear functions are shown in figure 22, while figure 23 shows the comparison of the shear wave velocity profiles. For the first 2m of soil, no shear wave velocity could be determined as there is no obvious linear correlation between the depth and shear wave travel time. This might be because at low depths, refracted waves might reach the receiver faster than the actual shear waves. However, the inability to determine a shear wave velocity in the first few meters below the ground is not particular to the slope method: while the other methods might formally provide a velocity, it can not be considered reliable for the same reasons. Three linear functions are fitted to the data corresponding to three soil layers in the borehole ground and the slope method provides reasonable shear wave velocities for the layers. In contrast to all other methods considered so far, the slope method is the only one without single unreasonably high velocities. This is probably mostly because measurements with obvious flaws have not been considered in the linear fit and small differences cancel each other out in the fit. Interestingly, the slope methods results in similar velocity profiles for both the depth - travel time data from the SPAS software as well as the cross correlation results which increases the credibility of the results further.

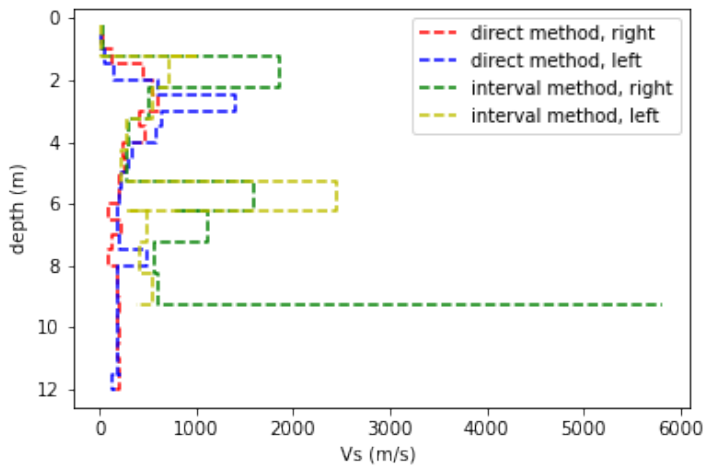


Figure 21: Shear wave velocity profile obtained with the direct and the interval method.

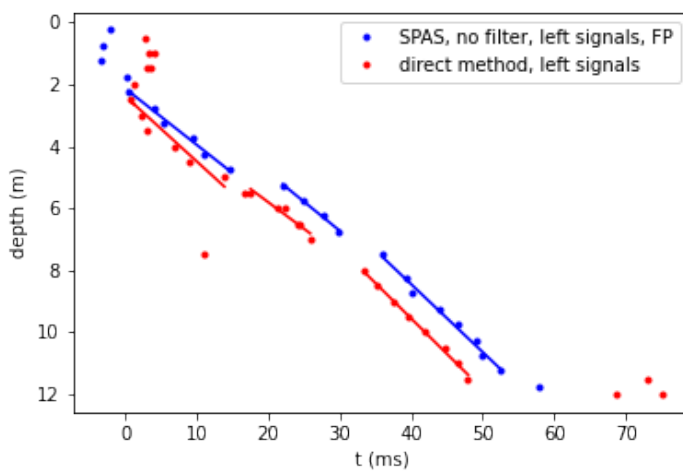


Figure 22: Depth - travel time profiles obtained by the SPAS software [27] as well as the cross correlation in python with the fitted linear functions for the slope method.

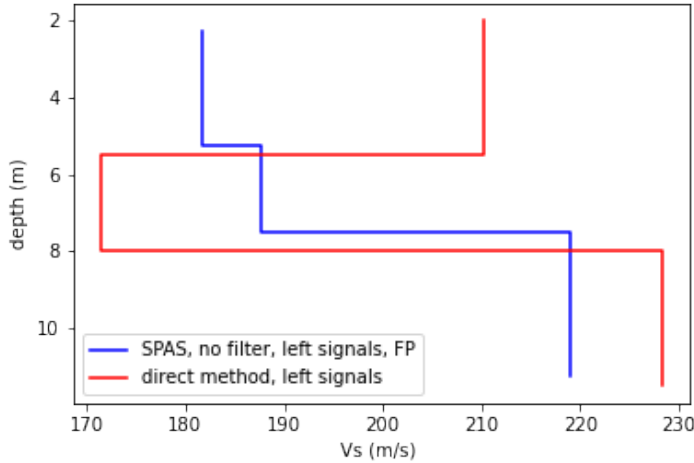


Figure 23: Depth - shear wave velocity profiles obtained with by the slope method.

5.3 Comparison of the different analysis methods

Figure 24 shows the depth - travel time profiles from the methods described above. The shear wave velocity profiles are summarised in figure 25 and 26. Overall, the slope method yields the most reliable results as there are no miscalculated points with unreasonably high shear wave velocities. Between the two data preparation methods the direct method seems to be more trustworthy as it does not rely on the "black box" SPAS software. Figure 27 compares the results for the slope method in combination with the direct method as the most reliable result with all other investigated methods. However, the slope method comes with the disadvantage of possible gaps in the velocity profiles (see figure 23), the necessity of an upstream data analysis to produce the depth - travel time plots, and the dependence of a manual assessment of the number of soil layers (number of linear functions fitted to the data) as well as the limits of those soil layers. It requires the most manual input and time. The direct method, which can be run mostly automatically by a python program, results in very reliable results as well, with the exception of a few miscalculated velocities, mainly in the higher soil layers where the data might not be reliable due to refraction effects anyway. In contrast to the slope method it has the advantage of not relying on a manual sorting of the data points. Surprisingly, the interval method, which was expected to be more accurate than the direct method [5], included some very high shear wave velocities. This might be the result of a higher sensitivity towards smaller layers of soil, but requires further investigation. As discussed in detail above, the SPAS software offers many possibilities for the analysis of the measurements. Since the internal algorithms of the analysis are not published and transparent, it is difficult to trace the analysis process and identify possible error sources. The most trust-worthy option seems to be the time-intensive manual identification of the first peak in each measured signal, whereas the semi-automatic or fully automated analysis are very prone to unreasonably large differences in the V_S estimates.

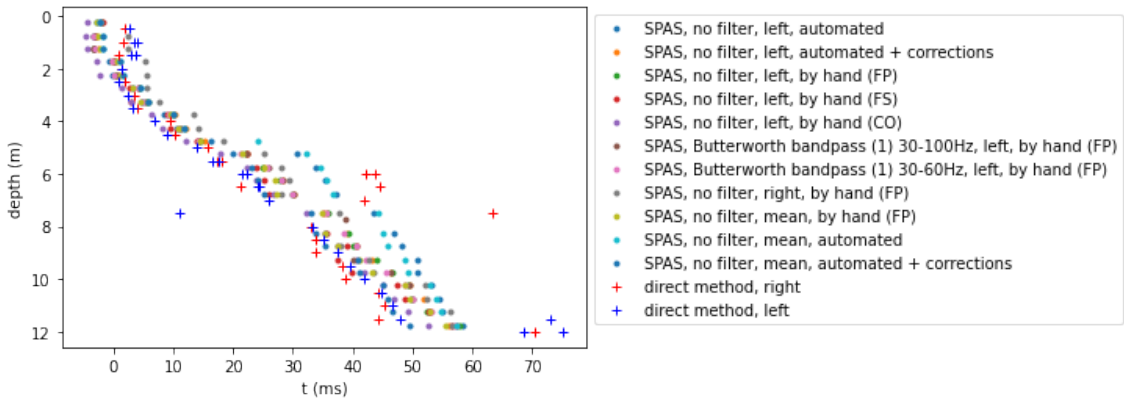


Figure 24: Depth - travel time profiles obtained by the different analysis methods.

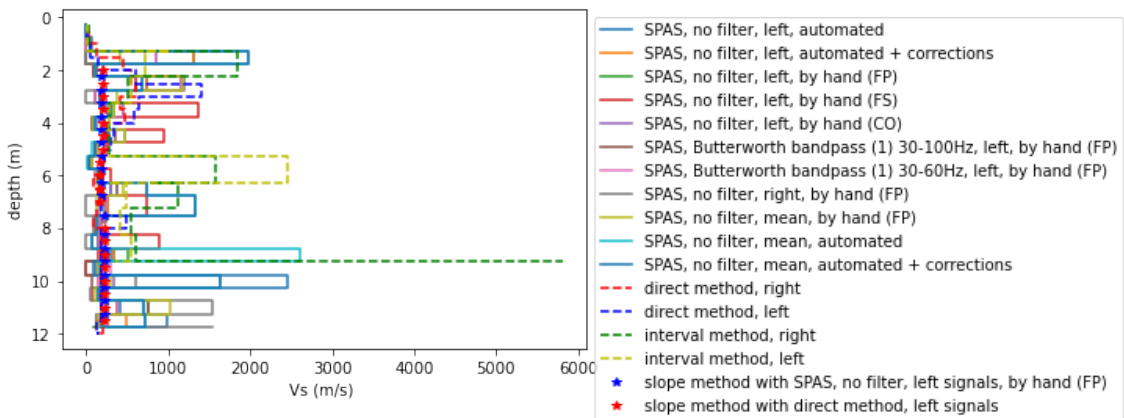


Figure 25: Depth - shear wave velocity profiles obtained with the different analysis methods.

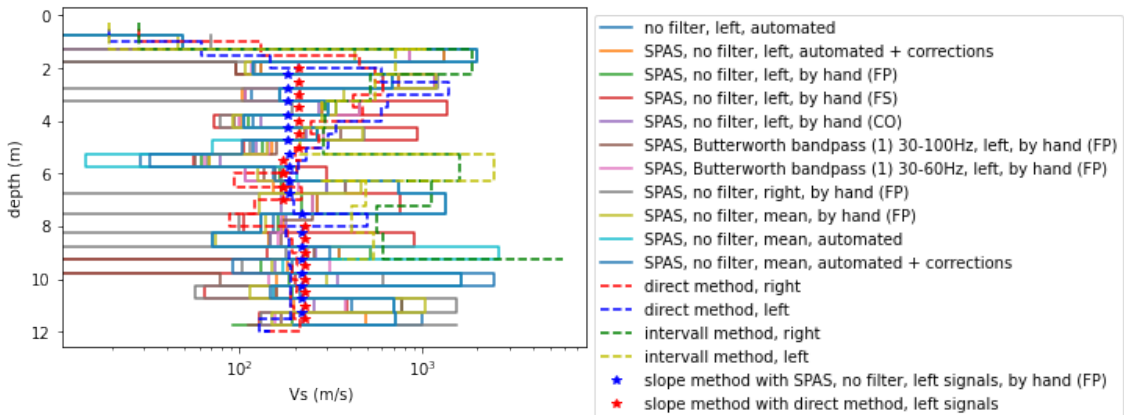


Figure 26: Depth - shear wave velocity profiles obtained with the different analysis methods on a logarithmic plot.

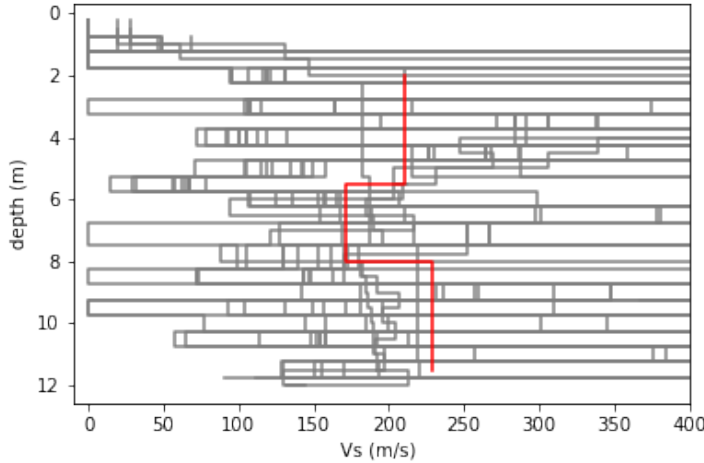


Figure 27: Depth - shear wave velocity profile for the slope method in combination with the direct method (red) compared to the other analysis methods.

6 Shear Wave Velocity Profiles from CPT-Data

A shear wave velocity profile can be determined via invasive and non-invasive testing methods as explained in section 2. Although these methods have different disadvantages in their use (non-invasive methods might not have an unique solution and the results will show a lowering resolution with increasing depth while invasive methods are generally more time consuming and expensive as they rely on boreholes and will only represent the velocity distribution at a single point rather than over a line or ground area), they generally provide the very reliable V_S measurements. An alternative technique for determining a shear wave velocity profile is by using the results from other geotechnical investigations like cone penetration tests (CPT) or standard penetration tests (SPT). Those methods are widely used to the point where databases with those measurements for a certain region might already exist which can be used as a starting point for determining a V_S profile, they are relatively inexpensive and yield several measured variables able to provide information not only on the shear wave velocity but also on soil type and profile, density, shear strength, the liquification potential,... [29]

The shear wave velocity can be estimated from CPT data using empirical correlations to the measured variables which were developed by comparing a measured V_S profile to the CPT data. Those correlations are often bound to a specific site and the respective soil conditions or are only applicable for certain soil types, but there are also some more general CPT- V_S correlations allowing for a V_S estimation regardless of the site specific settings, for example: [29]

The CPT- V_S correlation from Mayne (2006) correlates the measured sleeve friction f_s with V_S using: [30]

$$V_S = 51.6 \log_e(f_s) + 18.5 \quad (6.1)$$

In contrast, the correlation developed by MolaAbasi et al. (2015) also includes the measured cone resistance q_c : [31]

$$V_S = 100 [1.40 + 1.59f_s + 0.09q_c - 1.33f_s^2 - 0.002q_c^2 + 0.05f_sq_c] \quad (6.2)$$

The correlation developed by Robertson (2009) [23]

$$V_S = \left[\frac{\alpha_{\nu s} (q_t - \sigma_{\nu 0})}{P_a} \right]^{0.5} \quad (6.3)$$

$$\alpha_{\nu s} = 10^{0.55I_c+1.68} \quad (6.4)$$

relies on the soil behaviour type index I_c to account for differences in the soil types. [29, 32]

Hegazy and Mayne (2006) published a CPT- V_S correlation based on the normalized cone tip resistance Q_{tn} , the effective vertical stress $\sigma'_{\nu 0}$ and the atmospheric pressure P_a : [33]

$$V_S = 0.0831Q_{tn}e^{1.786I_c} \left(\frac{\sigma'_{\nu 0}}{P_a} \right)^{0.25} \quad (6.5)$$

In New Zealand, most research on CPT- V_S correlations has been done in the Canterbury region following the 2010/11 Canterbury earthquake sequence. McGann et al. (2015) developed a local relation between V_S and the sleeve friction f_s , the cone resistance q_c and the depth d : [34]

$$V_S = 18.4q_c^{0.144}f_s^{0.0832}d^{0.278} \quad (6.6)$$

Those five different general CPT- V_S correlations were implemented in python, in figure 28 the results for the V_S profiles are compared with each other as well as the shear wave velocities obtained with the CPET-IT software ³ used for analysing the CPT data. The six methods for obtaining an estimate of V_S differ significantly from each other and yield very different shear wave velocities and profiles. However, all resulting shear wave velocities are within a resonable frame, there are no obvious extreme over- or underestimations. Interestingly, the results from the correlation published by McGann et al. (2015) and the software output show very similar V_S profiles with only a small offset between them. This suggests that the correlation used by the software is quite similar to equation 6.6.

Figure 29 compares the different V_S profiles obatined from the CPT data with the best result from the direct mesurement of the shear wave velocity from section 5.3. All CPT- V_S correlations manage to capture the overall shear wave velocity profile in the soil with three different layers with the second soil layer between a depth of 5m and 7m having the smallest shear wave velocity and the soil below 8m having the highest measured V_S . However, there are significant differences in the absolute values of the resulting shear wave velocities: The correlation from Mayne (2006) seems to agree best with the directly measured V_S profile, followed by the relationship from Hegazy and Mayne (2006). However, the results from Hegazy and Mayne (2006)

³CPT interpretation software CPET-IT v.3.0 from Geologismiki

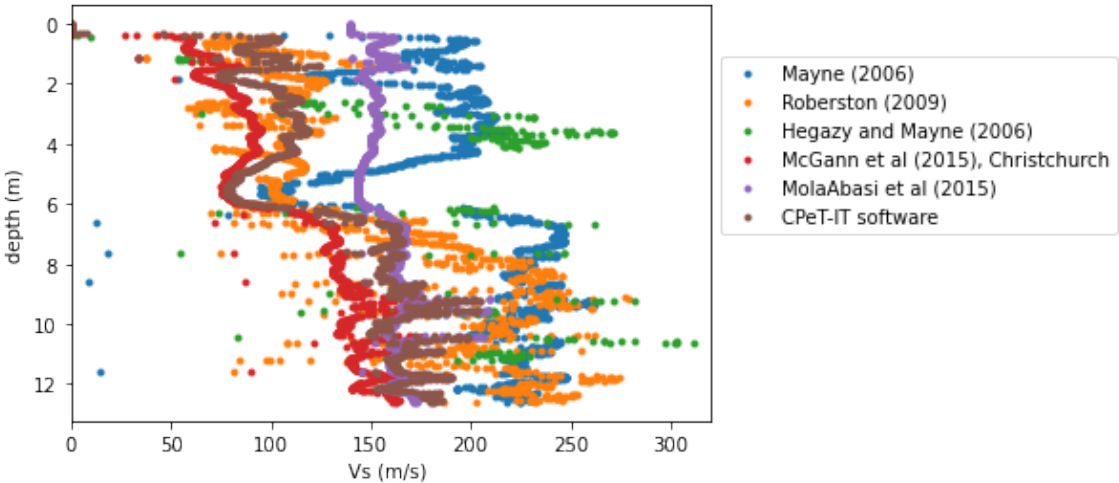


Figure 28: V_S profiles obtained from the CPT data with the different CPT- V_S correlations and as an output from the CPET-IT software [35].

show the highest fluctuations while the other correlations result in more even shear wave velocities for the three soil layers which can be assumed to be more reasonable. The equation from Robertson (2009) manages to capture the shear wave velocity of the third soil layer beneath a depth of 8m quite well, but falls short in giving a reasonable velocity for the other soil layers. The reason might be that although the CPT- V_S relation is meant to be able to describe all soils, it works better for the soil properties found in the third layer than in the ground above. Interestingly, all correlations fall short in giving a reasonable estimate for the second soil layer. The correlation by McGann et al for the Christchurch area as well as the software output generally describe the trend of the shear wave velocity in the ground quite well, but both underestimate V_S by a constant offset. Finally, the CPT- V_S relation by MolaAbasi et al (2015) seems to be quite unsuitable for calculation the V_S profile as it describes neither the profile nor the absolute velocity values correctly.

In summary, the CPT- V_S relation published by Mayne (2006) (equation 6.1) seems to be the most suitable to get an estimate for the V_S profile for the given data set. However, the comparison of different correlations underlines that V_S can only be estimated from measured CPT data as there are no direct causal relations. Empirical correlations might greatly differ from each other and their applicability might heavily depend on local soil conditions.

7 Relation between Liquefaction and the Shear Wave Velocity

Liquefaction is the process in which a solid soil changes its state and behaves like a fluid. It can occur during an earthquake in loose sand and silt soils below the water table where all spaces between individual grains are filled with water. Normally, the friction at the contact points would hold the soil together, but during the shaking

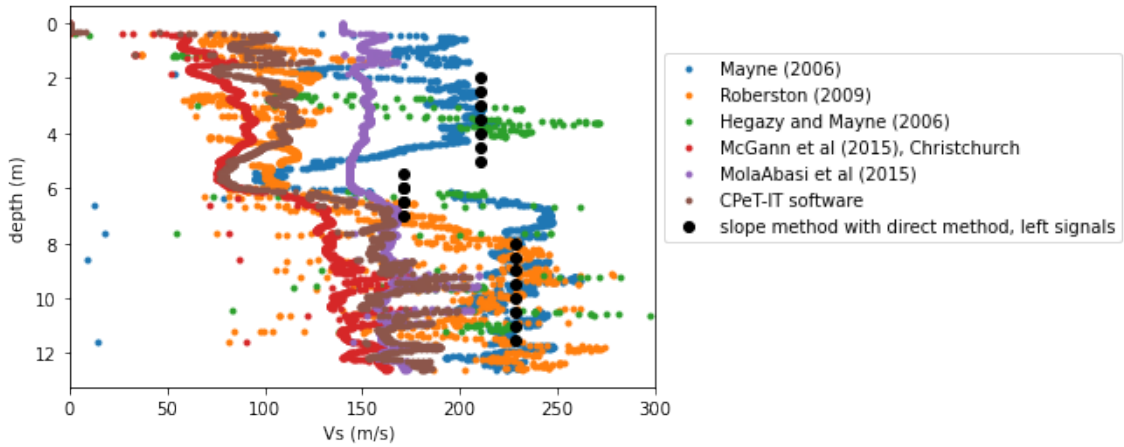


Figure 29: V_S profiles obtained from the CPT data with the different CPT- V_S correlations and as an output from the CPET-IT software [35] compared with the results from the direct measurement of V_S .

from an earthquake the individual grains get completely separated and the soil loses its soildity. The liquefaction potential of a soil is an important property to consider in earthquake-resistant design as liquefied soil might not be able to support the weight of overlaying soils or structures. [7]

The liquefaction potential of a soil can be predicted from variables measured in penetration tests like SPT or CPT. Besides, the shear wave velocity can be correlated to the liquefaction potential as both are controlled by the same soil characteristics like the soil type, density and stress. Due to the large extend of research on the correlation of penetration test results to the liquefaction as well as the existence of large databases these methods are generally preferred over predictions from the shear wave velocity. However, using the shear wave velocity as a liquefaction predictor has the advantage that V_S might be measured using a non-invasive method (section 2) and might yield results for soils where penetration tests might not provide reliable measurements. [36]

A common approach to evaluating the liquefaction potential from the shear wave velocity includes the calculation of the cyclic stress ratio (CSR), a corrected shear wave velocity and the cyclic resistance ratio (CRR). The CSR describes the cyclic loading applied to the soil by an earthquake, it depends on the (assumed) level of ground shaking as well as soil conditions. The stress-corrected shear wave velocity V_{S1} can be interpreted as the stiffness of the soil and is calculated by normalizing the shear wave velocity with the a vertical reference stress. The CRR is meant to express the resistance of the soil to liquefaction, it describes the CSR separating liquefying soils and non-liquefying soils for a given V_S (see figure 30). The CRR can be derived from V_{S1} and many different CRR- V_{S1} correlations have been developed for site and soil characteristics (see figure 31). [7, 36, 37]

CSR and CRR can be combined to yield the factor of safety F_S

$$F_S = \frac{CRR}{CSR} \quad (7.1)$$

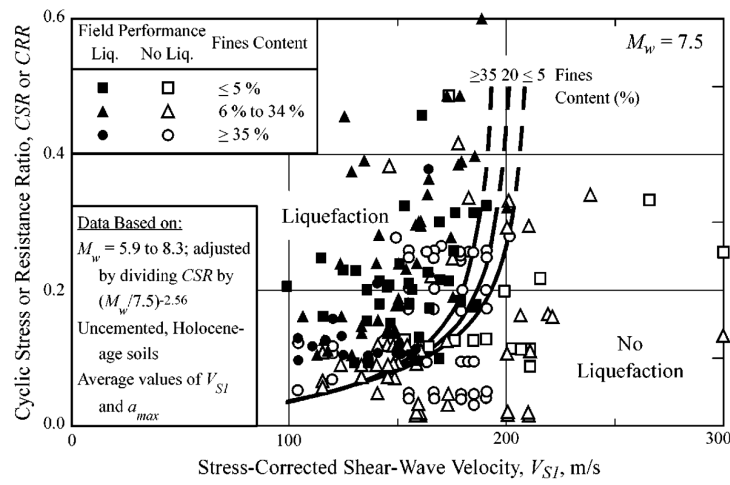


Figure 30: Liquefaction resistance curves (CRR- V_{S1} correlations) separating liquefying and non-liquefying Holocene soils for an earthquake with magnitude 7.5, from [36].

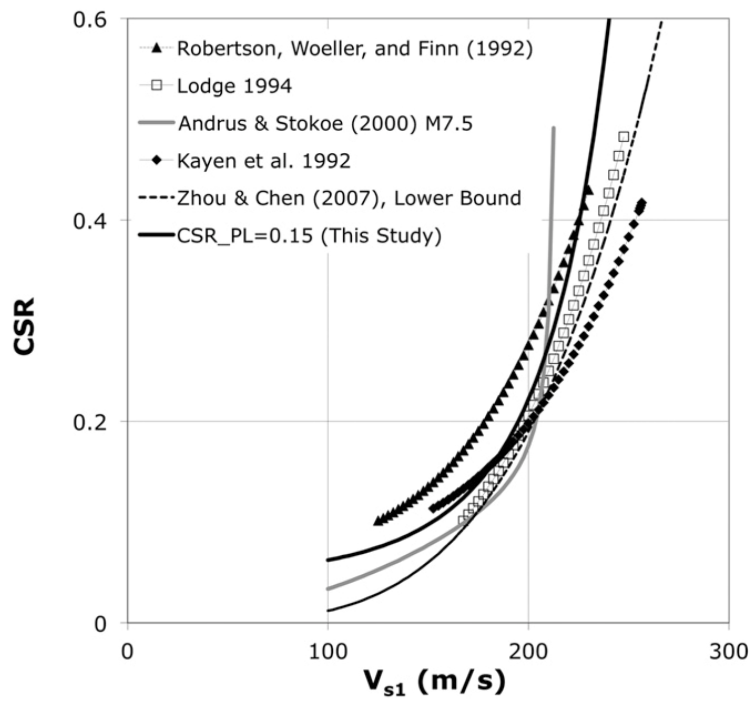


Figure 31: Different CRR- V_{S1} correlations, from [37].

which can be used to quantify the liquefaction potential of a soil: liquefaction is expected for $F_S \leq 1$, while $F_S > 1$ predicts no liquification during an earthquake. Alternatively, CSR and CRR can be evaluated using a probabilistic approach to determine a liquefaction probability which for example can be included in a risk evaluation for building design decisions. [7, 36]

8 Horizontal-to-Vertical Spectral Ratio

The Horizontal-to-Vertical (H/V) spectral ratio of seismic noise technique allows for a non-invasive determination of soil characteristics, especially the site fundamental resonance frequency. The correlated site period is used in New Zealand as the preferred variable for site subsoil classification (section 3.1), but it can also be used to estimate the shear wave velocity. The method relies on minimal equipment, uses passive sources, can be easily performed in urban areas and is relatively inexpensive and time-effective compared to other methods of site investigation (section 2). [3, 38]

H/V spectral ratios can be calculated from measurements of ambient noise, caused for example by traffic, wind interacting with structures, small earth tremors,... The recording made with a receiver placed on the investigated site will depend on the site soil characteristics, but also on the source of the tremor, propagation effects and the specifics of the recording instrument. Typically, the ground movement is measured in three directions: north-south, east-west and vertical shaking. Those measurements are then Fourier-transformed into the frequency domain. Dividing the horizontal signal, the combination of the north-south and east-west movement, with the vertical Fourier amplitude, will eliminate all effects from the source, the propagation and the receiver. The quotient of the Fourier-transformed signals of horizontal and vertical movement, also called the H/V spectral ratio, is therefore only affected by the site characteristics. Previous investigations have shown that the peak in the H/V spectral ratio corresponds to the fundamental site frequency. [38]

The most straightforward approach to evaluating H/V spectral ratio measurements directly implements the analysis procedure described above. More sophisticated analysis methods include different filters, data smoothing, resampling, frequency domain rejection algorithms and data analysis in individual time windows with the purpose of making the analysis more reliable, reproducible and minimizing the uncertainties on the final results. Two analysis systems are the Geopsy application⁴ and the hvsrpy python package⁵. [39, 40]

⁴Geopsy package, release 3.4.1

⁵jpvantassel/hvsrpy: v0.5.2 by Joseph P. Vantassel

Bibliography

- [1] W. Lowrie, *Geophysics: A Very Short Introduction*, **2018**.
- [2] Earthquake Commission, Invasive Seismic Testing - A Summary of Methods and Good Practice, **2019**.
- [3] S. Foti, S. Parolai, et al., *Surveys in Geophysics* **2011**, *32*, DOI 10.1007/s10712-011-9134-2.
- [4] D18 Committee, Test Methods for Downhole Seismic Testing, en, tech. rep., ASTM International.
- [5] L. David Suits, T. Sheahan, et al., *Geotechnical Testing Journal* **2004**, *27*, DOI 10.1520/GTJ11811.
- [6] S. Semmens, N. D. Perrin, et al., NZS 1170.5:2004 site subsoil classification of Wellington City.
- [7] M. A. Khan, *Earthquake-Resistant Structures: Design, Build, and Retrofit*, Elsevier, **2013**.
- [8] Standards New Zealand, *Structural design actions. New Zealand. Part 5, Part 5*, OCLC: 156766551, Standards New Zealand, Wellington [N.Z.], **2004**.
- [9] ASCE, Minimum Design Loads for Buildings and Other Structures, **2010**.
- [10] Building Seismic Safety Council, For New Buildings And Other Structures (FEMA 450), Part 1: Provisions, **2003**.
- [11] T. Thitimakorn, T. Raenak, *Open Geosciences* **2016**, *8*, DOI 10.1515/geo-2016-0046.
- [12] P. Anbazhagan et al., *Disaster Advances* **2014**.
- [13] Canadian Commission On Building And Fire Codes, National Building Code of Canada: 2005, en, **2005**.
- [14] European Committee for Standardization, Eurocode 8: Design of structures for earthquake resistance -Part 1 : General rules, seismic actions and rules for buildings, General rules, seismic actions and rules for buildings, **2004**.
- [15] A. Athanasopoulou et al., **2018**.
- [16] G. Forte, E. Chioccarelli, et al., Seismic soil classification of Italy based on surface geology and shear-wavevelocity measurements, **2019**.
- [17] A. I. Kanli, P. Tildy, et al., *Geophysical Journal International* **2006**, *165*, 223–235.
- [18] Erdbeben: Karten der Baugrundklassen, **2016**.
- [19] Code For Seismic Design Of Buildings, **2010**.
- [20] Indian Standard, Criteria For Earthquake Resistant Design Of Structures, Part 1 General Provisions And Buildings, **2002**.
- [21] Guia Boliviana De Diseno Seismico, **2020**.
- [22] Institute of Geological and Nuclear Sciences, 1:250 000 Geological Map of New Zealand (QMAP).

- [23] P. K. Robertson, *Canadian Geotechnical Journal* **2009**, *46*, DOI 10.1139/T09-065.
- [24] Tonkin and Taylor Ltd, **2015**.
- [25] Gisborne District Council, Tairāwhiti Maps, Version 4.2, **2020**.
- [26] Google, Google Maps, **2021**.
- [27] Geologismiki, Seismic Analysis Software SPAS 2019 v.4.0.
- [28] L. Wotherspoon et al., Assessing the quality and uncertainty of in-situ seismic investigation methods, NZGS Symposium 2021, **2021**.
- [29] C. R. McGann, B. A. Bradley, et al., *Soil Dynamics and Earthquake Engineering* **2015**, *75*, DOI 10.1016/j.soildyn.2015.03.021.
- [30] P. Mayne, *In-situ test calibrations for evaluating soil parameters*, **2006**.
- [31] H. Mola-Abasi, U. Dikmen, et al., *Near Surface Geophysics* **2015**, *13*, DOI 10.3997/1873-0604.2015010.
- [32] Rocscience Inc., CPT Data Interpretation Theory Manual, **2016**.
- [33] Y. A. Hegazy, P. W. Mayne, **2006**, DOI 10.1061/40861(193)31.
- [34] C. R. McGann, B. A. Bradley, et al., *Soil Dynamics and Earthquake Engineering* **2015**, *75*, DOI 10.1016/j.soildyn.2015.03.023.
- [35] Geologismiki, CPT interpretation software CPeT-IT v.3.0.
- [36] R. D. Andrus, K. H. Stokoe, et al., *Earthquake Spectra* **2004**, *20*, DOI 10.1193/1.1715106.
- [37] R. Kayen, R. E. S. Moss, et al., *Journal of Geotechnical and Geoenvironmental Engineering* **2013**, *139*, DOI 10.1061/(ASCE)GT.1943-5606.0000743.
- [38] S. M. T. Qadri, B. Nawaz, et al., *Earthquake Science* **2015**, *28*, DOI 10.1007/s11589-014-0105-9.
- [39] Geopsy, Geopsy package, release 3.4.1.
- [40] J. P. Vantassel, jpvantassel/hvsrpy: v0.5.2, en, **2021**.